

57p

4 OBSERVATIONS OF

THE WHITE LIGHT CORONA FROM A ROCKET

mfs
*4**
100
637
REF

A preliminary report of work conducted in preparation for OSO-B, supported in part by National Aeronautics and Space Administration Contracts S-14704-G and R-70.

NASA

UNPUBLISHED PRELIMINARY DATA

by

H. W. Cooper, C. R. Detwiler, M. J. Koomen, D. M. Packer,

J. D. Purcell, R. T. Seal, Jr., and R. Tousey

Feb. 1964 # 157p
ref

etal

H. Friedman
Chief Scientist

E. O. Hulburt Center for Space Research

U. S. Naval Research Laboratory

Washington, D. C., 20390

168 8944

GPO PRICE \$ _____

OTS PRICE(S) \$ _____

February 1964

Hard copy (HC) \$ 3.00
Microfiche (MF) \$ 0.50

FACILITY FORM 602

N65-19960

(ACCESSION NUMBER)

57
(PAGES)

CR-53537
(NASA CR OR TMX OR AD NUMBER)

(THRU)

1
(CODE)

28
(CATEGORY)

Encl (1)
to NRL ltr 7140-63
SER: 1519


ROLL

OBSERVATIONS OF THE WHITE LIGHT CORONA
FROM A ROCKET

INTRODUCTION

The white light corona is the faint and frequently irregular halo, extending from one to several solar radii from the limb, seen at the time of a total solar eclipse. Very close to the limb its brightness is about equal to the full moon, which can of course be seen during full daylight. Special instrumentation is required to observe the corona without the aid of an eclipse, however, because of the greatly increased sky brightness close to the sun, produced by forward scattering of sunlight by aerosols, and because of the difficulty of trapping instrumental stray light produced by the presence of the sun, whose brightness is 1 million times greater than the brightest part of the corona.

The brilliance of the sky, and of diffracted light is easily demonstrated by a rudimentary form of coronascope, consisting of the thumb and the eye. At arm's length, the thumb subtends about 1° , and is a convenient occulter with which to eclipse the sun and look at the sky close to



sun. Ordinarily what is seen is a whitish sky, of great brightness. From mountain tops, after a heavy rain has cleansed the atmosphere, or when pure arctic air has moved in, the sky may appear uniformly dark blue up to the very edge of the thumb. But then the edge itself shines with diffracted light, so brightly that the sun's corona is completely masked.

The corona consists of three components, called L, K and F. The L-corona comprises line emissions from highly ionized atoms; it extends only a few minutes of arc beyond the limb. The K-corona is sunlight scattered by the 10^6 degree electron gas; it is strongly polarized with electric vector tangential to the limb; its spectrum is like sunlight, but the Fraunhofer lines are almost entirely washed out by Doppler broadening. The F-corona is sunlight scattered by interplanetary dust; it shows the Fraunhofer lines; it is nearly unpolarized to elongations of about 15° , beyond which it merges into the zodiacal light and exhibits increased polarization.

The problem of observing the corona without the aid of a total eclipse was solved by Lyot in 1930 through the construction of a coronagraph which incorporated special features to reduce and trap the stray light originating from the sun. With this instrument the emission lines in

the L-corona, can be observed to extend several minutes of arc from the limb, when the sky is very clear and when the emission is intense. Observations of the K-corona with a coronagraph can be made to about 20 arc minutes from the limb. Since the K-corona is partially polarized, it can be studied with a polarimeter. Lyot (1929) was able to observe the K-corona to 6 arc minutes from the limb, using a visual polarimeter. More sensitive polarization photometers have been constructed, by Wlerick and Axtel, and by Dolfuss, but it is difficult to observe the K-corona to more than one solar radius from limb, except during a total solar eclipse.

The limitation to the usefulness of the Lyot coronagraph is caused by the earth's atmosphere which produces a bright sky whenever the sun can be seen. Figure 1, reproduced from van de Hulst shows the relative brightnesses of the several components of the coronal light, the daytime sky with and without haze, and the sky during a total eclipse. It can be seen that the clearest sky observed with the uneclipsed sun is about one millionth the brightness of the solar disc and swamps the corona within a few minutes of arc beyond the limb. During totality the sky brightness is reduced by nearly one thousand, as observed from the earth's surface, and this permits observing the corona to $R=4 R_{\odot}$.

Michard, by making observations at a wavelength near 6400 Å during the 1952 eclipse at Khartoum, was able to measure the F-corona brightness to $R=28 R_{\odot}$, because of the reduced sky brightness in the red. Blackwell approached the problem by photographing the corona during the 1954 eclipse from an aircraft at an altitude of 30,000 feet. The effective wavelength, 6300 Å, was also in the red. At this altitude the sky brightness was found reduced by a factor of 2 or 3 over the minimum brightness observed from the ground. Blackwell was thus able to observe the F-coronal brightness to $R=55 R_{\odot}$. Measurements were also made of the polarization.

Since the brightness of the sky is the reason why the corona can not be seen far from the limb with a coronagraph, it is obvious that a coronagraph placed above the earth's atmosphere would, in principle, make possible the observation of the white light corona at all times. At balloon altitudes, of the order of 30 km, the sky is reduced to a brightness nearly as low as that during a total solar eclipse. Above 100 km, however, except for possible airglow emissions, the sky brightness is effectively zero, and is only the brightness contributed by the stars themselves. Thus it is clear that the natural sky background offers no impediment to observations of the white light corona from rocket or orbiting vehicles.

On the other hand the design of a coronagraph to take advantage of the absence of sky light at orbiting altitudes, presents problems not encountered by Lyot. In the Lyot coronagraph the instrumental scattered light was reduced only to the level where it was negligible compared to the daytime sky brightness. A reduction by a factor of at least 1000 was required.

The obvious procedure is to prevent the direct light from the sun from entering the instrument by means of an external occulting disc. This has been done by several investigators. Evans constructed a small coronal photometer with an external occulting disc, for the purpose of measuring the brightness of the sky at approximately one arc minute from the sun's limb. The external occulter was placed 100 cm beyond the 3 mm diameter objective lens. With this instrument, he reported that the stray light brightness was approximately 10^{-6} of the average brightness of the sun, (B_s). Newkirk has stated that the level $10^{-8} B_s$ can be reached in the Evans photometer, but this value is about 100 times too great for a coronagraph that is to be used at altitudes above 100 km. Newkirk and Eddy constructed and flew from a balloon a coronagraph with an external occulter, but found the stray light level, $10^{-8} B_s$, was too great to permit

photographing the white light corona. Most of this stray light originated from sunlight diffracted from the periphery of the external occulter into its shadow. These problems have been discussed further by Newkirk and Bohlin.

THE CORONAGRAPH FOR THE ORBITING SOLAR OBSERVATORY

The Orbiting Solar Observatory (OSO) of the National Aeronautics and Space Administration offered the possibility of placing a white light coronagraph in orbit and monitoring the white light corona at frequent intervals. Design and construction of an instrument for this purpose was initiated in a proposal to NASA, dated 13 March 1961 and funded by NASA Contract S-14704G dated 20 July 1962. The principal limitation was one of space since the section of OSO providing pointing at the center of the sun to within 1 arc minute measured only 36 x 4 x 8 inches. A Lyot coronagraph with an external occulting disk was designed to fit into this space. It was necessary, however, to place the external occulter in position after launch and injection into orbit. This presented some difficulty, since the external occulter had to be precisely positioned. The 36-inch length of the box limited the length of the spar on whose end the occulter was fixed to considerably less than 30 inches. The OSO

coronagraph was small enough so that it could be flown in an Aerobee-Hi rocket for test purposes. This was accomplished on 28 June 1963. The present paper describes the characteristics of the coronagraph and presents a preliminary report of the findings.

The optical system of the OSO coronagraph is shown in Figure 2. Basically, the instrument is a Lyot coronagraph, equipped with an external occulter, and arranged for scanning of the image and photoelectric detection. The objective lens is of 25 mm diameter and 30 cm focal length, and was specially prepared so as to be as free as possible from defects that would produce scattering. An achromatic lens, placed in the focal plane, imaged the aperture stop B, on the diaphragm B' . This lens and diaphragm were introduced by Lyot, to trap the light diffracted from the edge of B. A triplet lens surrounding B' reimaged the corona on the plane of the scanning disc. Finally, a large lens placed behind the scanning disc imaged diaphragm B' on the aperture C' , placed directly in front of the photomultiplier, thus insuring the collection of all the light passing through B' regardless of the position of the scanning aperture. The lenses were computed and constructed by Tropel, Inc., Fairport, New York.

The external occulter was located 20 inches in front of the objective lens. This was the maximum distance compatible with the mechanism required to erect the spar. The photomultiplier was an Ascop 541a end-on type, having an S-11 surface. The response of this photomultiplier was similar to that of the light-adapted eye; thus the coronal measurements were made with white light. An additional stop, A', was placed in the position conjugate to A, in order to trap light diffracted from the periphery of A and reflected from the back side of A. To reduce this reflection, the rear side of the occulter was originally made in the form of a concave polished black glass mirror with center of curvature at the center of aperture B. This imaged aperture B back on itself, and since aperture B was the darkest part of the system, served as an effective trap for light originating from the earth or from the end of the box. In the flight unit, however, a plane, polished black epoxy surface was used, with equal or greater effectiveness.

A second coronagraph was also flown in the Aerobee rocket. This utilized a photographic film, rather than scanning and photoelectric recording. It was identical to the instrument just described, but with photographic film replacing the scanning disc and photomultiplier.

The scanning discs are shown in Figure 3. One disc was cut with a spiral slot, of width increasing outward linearly with distance. The second disc had a pair of radial slots of angular width, 2° , set opposite one another. Spur-gear teeth were cut on the periphery of each disc, but the one disc had one more tooth than the other. Both were driven from the same spur gear. As a result, the crossing point of the spiral and radial slots circled outward in a spiral fashion and scanned the corona with an aperture which was approximately $1/2 \times 1/2$ arc minute near the sun's limb, and grew to 5×5 arc minutes at $R=10 R_{\odot}$.

The field covered by both the photoelectric and photographic coronagraphs was from $R=3$ to $11 R_{\odot}$. It would have been desirable to record the corona much closer to the sun's limb, but this was not found possible for several reasons. First, the external occulter, in the form used, produced considerable vignetting. This could have been greatly reduced by placing the occulter at a greater distance from the objective lens, had space been available. Second, it was necessary to allow safety factors to take care of the possibility of misalignment and errors in pointing.

In the photoelectric coronagraph polarizers were provided to make possible the measurement of coronal brightnesses in both tangentially and radially polarized light.

This was done by placing glass-laminated Polaroid over the one radial slot, with transmission direction radial, and similar Polaroid over the second radial slot, with transmission tangential. In operation, the corona was first scanned with the one radial slot, then scanned with the other slot, thus providing records in each direction of polarization.

OCCULTERS

The key to the operation of this coronagraph is the occulter. As previously mentioned, using a smooth-edged occulter, Evans was able to reduce the stray light to $10^{-6} B_s$, and Newkirk states that 10^{-8} can be reached. It was necessary, however, to reduce the stray light to approximately $10^{-10} B_s$.

Since the source of stray light is the diffraction from the edge of the external occulter, it would be possible to reduce this by the interposition of additional occulters behind the first, arranged in such a way that the objective lens would not see the edge of any but the nearest occulter. Consideration was given to use of a multiple-disc occulter of this type, but the mechanical difficulties of placing more than one disc in position after injection into orbit with severely limited space for the mechanism, made this

solution impractical. The use of a multiple-disc occulter for a coronagraph was independently investigated by Gillette, who reported reducing the stray light level by 10^4 , using three occulting discs instead of one. Newkirk and Bohlin (1963) have independently investigated the multiple occulter, and with a triple occulter reached a reduction in the stray light by a factor of approximately 13 only. More recently, Newkirk and Bohlin (1964) have completed the construction of a coronagraph with a triple occulter. The stray light was found to be $1.1 \times 10^{-9} B_s$ over the entire field to $5 R_o$ with a Lyot aperture limiting the inner boundary to $R=1.7 R_o$.

The occulting disc used for OSO-B and for the Aerobee rocket experiments was made in the form of a toothed disc as shown in Figure 4, a diagram, not to scale, showing the direction in which the light is diffracted from a group of teeth. As described by Purcell and Koomen (1962), each tooth may be thought of as a pair of straight edges and point intersections. Parallel light incident normally to the plane of the figure is diffracted in a direction at right angles to each edge, as shown. Thus the diffracted light forms a circular envelope within which no light is permitted to enter. For this condition to be realized, however, the edges must be absolutely clean and free from any irregularities, and the points and valleys between teeth must be sharp.

Figure 5 is a photograph of the diffraction behind a single V-notch analogous to the saw-tooth. A point source was set up some distance away and photographic film was placed 24 inches behind the notch. Three exposures are shown. It is clear that almost all the light is diffracted at right angles to the two edges. The streaks in the pattern are caused by lack of perfect smoothness of the edges, although they were well-sharpened razor blades. In principle, some light should be diffracted more or less circularly from the point, but no light from this source was detected.

In Figure 6 reproductions are presented of exposures made with a point source illuminating, in the one case, a disc with a smooth edge, and in the other, a disc with 240 teeth. The photographic film was 24 inches behind, in each case. The short exposures, on the left, show the geometrical shadow of the two discs; the individual teeth can be seen to be surrounded by a bright edge; the straight sides of the supporting post and the edge of the smooth disc are bounded by interference bands, lying outside their geometrical shadows. In the long exposures, it is possible to compare the effectiveness of the two types of occulter. In the case of the smooth disc, it is obvious that much light was diffracted into the shadow. Although the diffracted intensity

decreased rapidly with angle, it was still sufficient to produce the bright spot at the center where the total from the entire periphery comes to focus. The radial streaks were produced by irregularities on the periphery, which distorted the wave front, locally. Since the support for the disc lay between the disc and the light source, it shaded a section of the edge of the disc from the source. Therefore no light was diffracted in the radial direction over this portion of the periphery. The fact that the shadow cast by the support was dark, shows that much light was actually present throughout the shadow. In the case of the toothed disc, however, the shadow of the supporting post cannot be seen, hence there was almost no light within the shadow. The shadow cast by the toothed disc is smaller in diameter than the disc itself, but has a sharp edge, as would be expected from the form of the envelope produced by rays diffracted from the teeth, as shown in Figure 4. The shadow of the smooth disc does not have a sharp edge, and is smaller than the disc because of the overexposure.

Figure 7 is a photograph of each type of disc, illuminated with a point source, but made with a camera situated behind the disc with lens entirely within the shadow. The camera was focussed on the disc. It is evident that the

smooth disc produced a bright ring of diffracted light. In the case of the toothed disc the individual teeth are visible, with certain exceptions. This was caused by the fact that it is almost impossible to clean the teeth sufficiently to prevent some light being diffracted by small points of foreign matter along the teeth. Careful inspection, however, shows that a few teeth appear to be completely absent, showing that they were especially clean.

Figure 8 shows photometric measurements made with a photomultiplier. The discs were illuminated with a point source, and the light behind the disc was measured with a photomultiplier situated behind a movable pinhole. In the case of the smooth disc the light diffracted into the shadow was intense and built up to a strong central spot. For the toothed disc however, the intensity in the central region of the shadow was reduced by more than an order of magnitude, relative to the minimum intensity behind the smooth disc. Considerable light, however, was diffracted beyond the boundaries of the envelope defined by the rays diffracted at right angles to the teeth, which was located at the 19 mm position. This is believed to have been caused by the fact that this experiment was conducted in the air, and scattering from the inevitable dust, which is strong in the forward direction, filled in the shadow outside 12 mm. This measurement is to be repeated in vacuum.

Newkirk (1962), and Newkirk and Bohlin (1963) have criticized the above explanation of the action of the toothed disc and say that it is best thought of as a form of apodization. They state, further, that it can be treated theoretically by diffraction theory, if it is replaced by a disc whose transmittance varies radially across the edge in accordance with the average transmittance function of the teeth. This type of approximation is not valid. It would be possible, of course, to treat the toothed disc by diffraction theory, but it would be necessary to preserve the toothed form, and integrate over each toothed opening. Whether the toothed disc is considered a form of apodization or not, depends upon the definition of this term. If apodization is interpreted so broadly as to include any change in form of the wave front produced by manipulation of the edge, the toothed disc might be properly termed a apodization. It is clear, however, that the operation of the toothed disc is most simply explained by Figure 4. Its action is not simply to eliminate the central spot, which carries only a small portion of the light diffracted within the shadow and into the objective lens of the coronagraph; it also prevents all the diffracted light from entering the entire objective lens.

The production of a suitable toothed disc was accomplished in the following fashion. Discs were first cut from 0.002-inch thick spring steel. A number of blanks were clamped together and mounted on a mandril in a milling machine. Very carefully and slowly, with a suitable cutter, teeth were ground around the periphery of the blanks. The profile of each tooth was 30° and each disc was cut with 180 teeth. The valleys between the teeth had rounded profiles, of course. After removal from the machine, two discs were combined so that the teeth overlapped, thus producing a disc with 360 teeth and with very sharp valleys between adjacent teeth. The major problem, however, was in cleaning the teeth. Each tooth was first cleaned by hand with a small tool, to dislodge burrs and so forth. Then the disc was mounted on the spindle of a drill press and immersed in a beaker containing water, detergent, and fine pumice. After spinning for some time in this solution, the disc was removed, washed, and dried, and found to be reasonably clean. Other methods, such as supersonic vibration and chemical cleaning, were relatively ineffective.

It was essential, of course, to assemble the coronagraphs under the strictest conditions of cleanliness. This was done in a clean-box. The entire unit was sealed. After

evacuation in flight, a cap, covering the stowed occulters and objectives, was thrown off and the spar placed in position.

CALIBRATION OF THE CORONAGRAPHS

Both the photoelectric and photographic coronagraphs were set up, adjusted, and tested in a vacuum chamber. This was necessary in order to eliminate the scattered light introduced by the air and the aerosols that it contains. The vacuum tank was 3 ft in diameter and 25 ft long, and was provided with baffles so as to be completely black inside. At one end, an artificial sun was introduced. This took the form of a tungsten lamp with a ribbon filament, imaged on a circular aperture, which in turn was placed at the focus of a lens. This lens was of a large enough diameter so that the parallel beam it projected down the vacuum tank covered the end of the coronagraph. Its diameter was such that it subtended at the coronagraph 32 minutes of arc, and so simulated the sun. Since the lens was not at infinity relative to the coronagraph, a slightly different adjustment of the coronagraph was required when in the tank than in flight. The brightness of the artificial sun, of course, was far below that of the actual sun, but the brightness was known and the factor was taken into account in all the calibrations.

An artificial corona was set up in the tank. This comprised a set of plaques of different and adjustable brightnesses, covering the range from 10^{-6} to $10^{-10} B_S$. Under these conditions it was found possible to reduce the stray light in the coronagraphs to the level $2 \times 10^{-10} B_S$, a value not quite as low as desired, but of the order of magnitude of the coronal brightness expected at $R=10 R_\odot$.

The calibration of the coronagraphs was accomplished in the vacuum tank by presenting a uniformly bright field of view. The calibration curve for the photoelectric coronagraph is shown in Figure 9, which gives the photocurrent output, as a function of R/R_\odot , for a uniform surface of brightness $1.4 \times 10^{-8} B_S$. The light emitted from this surface was unpolarized, and the curve was the same for both radial and tangential scans. A similar curve is shown in Figure 10 for the photographic coronagraph, but here it was derived by calculation. In the photographic instrument, the increase in brightness with R was caused by the vignetting action of the external occulter, which was very strong at $R=2 R_\odot$ and was still present at $R=10 R_\odot$. In the photoelectric instrument the same vignetting function was present; in addition there was the change in scanning aperture with R , resulting in an area $\propto R^2$. Therefore the total vignetting was much greater than for the photographic instrument.

The effect of the vignetting, in the case of the photographic coronagraph, was to compensate quite closely the decrease in coronal brightness with R . In the photoelectric coronagraph the vignetting was excessive, as can be seen from the curve showing the actual current recorded from the solar corona on 28 June 1963.

The stray light level is shown in Figure 9 by a curve of output with the artificial sun in operation. Compared to the output for the uniform surface of $B=1.4 \times 10^{-8} B_s$, at $R=10 R_\odot$ the stray light level was about $10^{-10} B_s$, but at $R=4 R_\odot$ the value was $10^{-9} B_s$. Compared to the current measured with the actual corona, however, the stray light signal was negligible.

OBSERVATIONS OF THE CORONA

One photoelectric and one photographic coronagraph were flown in an Aerobee-Hi rocket from the White Sands Missile Range on June 20, 1963, and a second pair of instruments were flown on June 28, 1963. On the first date the instrumentation was mounted in an SPC-400 pointing control manufactured by the Ball Brothers Research Corporation. The second flight made use of the large-type pointing control of the University of Colorado. The data from the first flight were only fragmentary because the telemetry did not function properly, and because the parachuted instrument was not ever found. The results from the June 28 flight however were excellent. A complete series of photographs were secured with the one instrument and two complete scans of the corona with the other. The sun was at a zenith angle of about 70° .

Photographs of the Corona

With the photographic coronagraph 23 exposures were obtained with exposure times between one second and 56 seconds, using Eastman Kodak type I-D spectroscopic emulsion. The pertinent data are presented in Table I. In Figure 11 all the pictures are reproduced, at approximately the same size as the originals. The shadow cast by the occulter and by the post supporting it is conspicuous. Each photograph

Table I

Exposure No.	Time from takeoff to middle of exposure (sec)	Altitude of middle of exposure (Km)	Exposure time (sec)	Relative angle of rotation (degrees)	Notes
1	116	131	2.0	+30	reduced to intensities.
2	118	133	1.1	+30	good -tracks.
3	122	137	7.0	+29	double exposure with 4 and tracks.
4	131	149	14.0	+25	double exposure with 3 and tracks.
5	140	157	3.8	+19	tracks; but corona visible.
6	142	160	2.0	+17.5	mostly tracks.
7	144	161	1.1	+15.5	tracks, but corona visible.
8	148	165	6.7	+12.5	tracks, but corona visible.
9	166	179	27.6	- 2	mainly tracks.
10	188	191	13.9	-12	some tracks - but useful.
11	197	195	3.86	-12	reduced to intensities.
12	200	197	2.0	-11.5	good.
13	203	198	1.1	-11	blotchy development.
14	223	203	34.8	+ 4.5	mostly tracks.
15	238	204	3.8	+18	tracks, but corona visible.
16	241	204	2.0	+20.5	tracks, but useful.
17	242	204	1.1	+21.5	good.
18	246	204	7.0	+24.5	tracks, but corona visible.
19	278	198	55.8	+28	mostly tracks.
20	308	185	3.8	+ 7	reduced to intensities.
21	311	182	2.0	+ 5	tracks.
22	312	181	1.1	+ 4	probably fogged and tracks.
23	320	173	16.2	- 1	much fog and tracks.

has been oriented with solar north at the top and east at the left. Since the yaw cone of the rocket during flight resulted in a rotation of the coronagraph around the optic axis to the sun, the shadow cast by the post changed in position relative to the sun. The angle was worked out from the aspect information from the rocket obtained by the University of Colorado from a study of the magnetometer data, and from the position potentiometer which gave the elevation angle relative to the rocket axis. The angles between the center of the post and solar east are given in Table I, for the middle of each exposure, and the angular motion of the center of the post is indicated in Fig. 11.

On examining the photographs several kinds of defect are immediately apparent. First, there is a bright region at the edge of the occulter about 120° from the post. This was produced by misalignment of the instrument in azimuth through approximately two minutes of arc. During the flight the alignment error decreased, and in the last exposure only a small amount remained. This light was not direct sunlight, but only light diffracted by the occulter teeth into the envelope, shown in Fig. 4, which was supposed not to enter the objective. The circular character of the envelope can indeed be seen on each

photograph as a sharp boundary to the shadow. Previous tests in the vacuum tank showed that misalignment of this magnitude did not throw appreciable scattered light over the entire field, but only into this particular region, close to the occulter. Therefore, this source of stray light did not invalidate the entire picture.

The second type of defect is the presence of a large number of bright spots, most of them not sharp, but at the same position on each photograph. These were not present before flight. They were produced by dirt, shaken loose during the vibration period associated with propulsion, and coming to rest on the Lyot field lens. They were illuminated by the corona and the light coming past the edge of the occulter. Most of these simply scattered, a few however, were opaque. There is visible also an opaque object that must have been on the film, since its position changed from exposure to exposure and its outline is sharp. This object is visible in Exposures 8 through 11, and again in 14 and 15, 20, 22 and 23. It was probably held electrostatically, but jumped from place to place during film transport. These blemishes destroy the smooth appearance that the corona pictures should have had, but they do not affect the pictures in any other way.

Third, in Exposures 3 and 4, there are overlapping images. These were caused by faulty film transport. Actually, Exposure 4 overlapped Exposure 3, but it has been printed separately.

Fourth, there are present in many of the exposures large blobs of light, frequently with well-defined, curved edges. There are also present many kinds of streak, some curved, some straight, some sharp, and some out of focus. At first the origin of these streaks was a source of great concern, and it was doubted that any data of significance could be derived from the photographs. On further examination, however, it was obvious, that these artifacts were real objects floating in space and illuminated by sunlight. The sharp objects were far from the rocket, so that they were in focus on the film. The large, broad light streaks and exposed areas were produced by objects so close to the objective lens, as to be far out of focus. In many cases these tracks can be seen to enter the field, then can be followed from exposure to exposure and finally seen to leave. The angular velocities were usually small, of the order of tenths of a degree per sec. All the conspicuous tracks are indicated in Fig. 11 by lettered arrows, showing the positions of entering and leaving the field. For

example, in Exposure 19, at the north, there is a sharp curved track, indicated by an arrow and letter x, which is seen continued in Exposures 20, 21, 22, and in 23 passes off the edge of the field. The object must have been rotating several times per second since the line is wavy. Apparently it was moving at nearly the same velocity as the rocket, since its angular velocity was about $0.02^\circ/\text{sec}$ relative to the line from the rocket to the sun. The sharpness of the track shows that the object must have been several hundred feet away from the rocket. Assuming a distance of 100 M, its velocity component in the plane normal to the direction to sun was about 3 cm/sec. Possibly it was one of the doors. However, the doors were thrown off several minutes earlier, at an altitude of approximately 70 km and it seems most improbable that one of these would have been in the field of view. Also present in Photograph 19 is another track in the east, labelled y, having much the same nature and disappearing in the region of the external occulter; it is seen emerging again in Photograph 22, and in 23 continues and leaves the field. Still another, entering 19 at the south and noted by w, leaves in 23. This object is closer; judging from the path width, the distance was 10 M. Its speed works out to be 5 cm/sec. Not all these tracks could have been doors. It is difficult to

to explain objects of this sort, showing long persistence and moving with the rocket, but at such a great distance. The close-by objects however could perfectly well have been caused by loose material of some sort coming from the rocket. It would take only a small flake of paint, for example, to throw a great deal of light into the region of the sky covered by the coronagraph, since it would be illuminated by full sunlight. An analysis of these paths is in progress. The objects appear to be moving too slowly to be of meteorite origin.

The question may be raised whether these particles could possibly have been inside the coronagraph housing. It is impossible to explain them in this way. The particles in sharp focus could not have been floating in the coronagraph, since it is most unlikely that their paths would have remained in a plane such that they would stay in perfect focus, and only two such planes exist within the instrument. The large particles and blobs of light are believed to lie outside because there was not sufficient light inside the instrument to illuminate them to this extent.

The presence of these large blobs of light resulted in a number of photographs being useless, as indicated in

Table I. However, the in-focus trails are of no consequence, and were easily avoided in the reduction of the photographs to obtain intensities.

In Fig. 12 Exposure 11 is reproduced, together with a retouched version of this exposure. All blemishes were removed in so far as practicable, including the light streak from misalignment. The shadow of the occulter was made somewhat larger than necessary. Introduced into the center of the occulter shadow and at the correct scale is a photograph of the solar corona obtained during the total eclipse of July 20, 1963, by Firor and others of the High Altitude Observatory. It has been oriented correctly relative to the rocket corona picture. This was obtained 22 days later than the rocket picture. Since the synodic rotation period of the sun is approximately 27 days, the rocket photograph was made with the sun rotated about 30° from its position on July 20.

Perhaps the most conclusive evidence that the photographs of Fig. 11 are the sun's actual corona comes from a comparison with the photograph at the lower right corner of Fig. 11. This was made before flight with the instrument in the vacuum tank, and with a uniformly bright light source. Here the photographic density decreases rapidly with

increasing R, as would be expected from the vignetting function, plotted in Fig. 10. In the flight exposure, however, there is no obvious change of density with R, just as would be expected from the curve of Fig. 10, calculated for the corona.

There is no suggestion of coronal streamers in the photographs of Fig. 11. However all the pictures show greater brightness in the direction of the sun's equator, and the approximate direction of the earth's ecliptic, than in the direction at right angles. This is in part, of course, the zodiacal or F-corona. It appears probable however, that a portion is true K-corona, because the brightness over the sun's south pole was greater than over the north. The pictures taken during the total eclipse also show greater brightness over the south than the north polar region. The zodiacal corona on the other hand is expected to be symmetrical from north to south.

It can be seen from Fig. 11 that increased brightness in the equatorial region was present on all the pictures where artifacts did not cover it up. Although the post position changed relative to the solar coordinates through a total of 42° , due to the rocket yaw cone, the equatorial region of increased brightness remained in the correct

position. For example, comparing Figures 1 and 11 one sees the increased region of brightness in the west on both exposures. In the east however, although the post was in the way, the region of increased brightness can be seen at the north side of the post in Exposure 1, and at the south side of the post in Exposure 11.

The question arises whether a day airglow emission may have contributed appreciably to these pictures. The densities of the several exposures have been compared with the exposure times, making allowance of course, for the artifacts. The result was a fairly smooth curve of density vs. log exposure time. The points did not depart from the curve in a consistent fashion, as they would if there had been appreciable airglow emission in the region traversed, between 130 and 204 km. There is however, no way to determine whether some of the emission may have been produced by airglow above the peak of the flight.

The corona photographs were of no value closer to the sun's limb than $R = 3.5 R_{\odot}$. This is a little beyond the outermost part of the corona photographed during the July 20, 1963 eclipse. It was a disappointment not to be able to photograph closer than this to the limb, but this was a result of the short distance to the occulter, as explained earlier.

Coronal Brightness Derived from the Photographs

Photographs 1, 11 and 20 were reduced to intensities by means of photographic photometry. In Fig. 13 the average isophots obtained from these exposures are reproduced. Since Exposure 11 was made with the post at 40° from Exposure 1, it was possible to fill in the shadow cast by the post, and this region is shown with broken lines. The equatorial brightness is greater than the polar brightness by a factor which in certain positions is as great as 2. These brightness values, given in ft.-Lamberts, may be converted to fractions of B_s by multiplying by 1.4×10^{-9} .

Average values taken from these isophots are plotted against R/R_\odot in Fig. 14, with brightness values given as fractions of the average brightness of the solar disc. It can be seen that the brightness values are slightly greater than the data from van de Hulst for the solar maximum or minimum. The results obtained by Blackwell during the 1954 eclipse, by photography from an aircraft are plotted in Fig. 15. From 6 to $10 R_\odot$ the equatorial brightness was found to be greater than the polar brightness by nearly a factor of 2. This is in fair agreement with the rocket results which show the equatorial brightness to be greater than the mean polar brightness by approximately 50%.

During the 1954 eclipse, however the Zurich sunspot number was nearly zero, since this was near the quietest part of the solar cycle. On June 28, 1963, the Zurich sunspot number was approximately 30, hence the sun was more active. This may account for the fact that our photographs show a difference between the north and the south polar regions and Blackwell's do not, and that our data show less difference between equator and poles than Blackwell's.

An important difference between the coronagraphic observations, and eclipse measurements is that in the former the entire outer atmosphere above the rocket is illuminated by sunlight, while in the latter it is not. Meteorites, and dust, therefore, will contribute their full share to the observed brightness. No estimate of the importance of this source of luminosity has been made, but it certainly must be considered as a possible reason for the greater brightness observed from the rocket coronagraph than has been recorded from ground during solar eclipses.

The Results obtained with the Photoelectric Coronagraph

The photoelectric coronagraph completed two scans during the time available, first in tangential and

second in radial polarization (vibration). After reduction of the telemeter records with the aid of the laboratory calibration curves and the rocket aspect solution, isophots were prepared, as shown in Fig. 16. They were plotted from points taken every 20° in azimuth. The regions affected by the out-of-focus image of the occulter support were not included, but it may be possible to carry the isophots a little farther into the shadow. The isophots are neither as smooth as one might expect, nor do they show any clear cut features, such as streamers. The irregularities were partly produced by the electrical noise present in the telemeter record, and partly by the foreign matter known from the photographs to be flying through the field of view. However, the general shape and the radial distribution are in agreement with the photographic record, as can be seen by comparing Figures 13 and 16. The brightness values for each set of photoelectric isophots refer to the brightness of an unpolarized corona. To obtain brightness values that can be compared with those of Fig. 13, the brightnesses of the radial and tangential components must be averaged, not added.

From the isophots, curves of brightness, averaged in azimuth were derived as functions of radius, for each

component. These are plotted in Fig. 15, together with the curve from Kuiper, for the average from equator to poles for solar maximum. Also shown are Blackwell's data for the K + F coronas at close to solar minimum,

The values of total brightness, given by the mean between the radial and tangential curves, are higher than the photographic value at $R = 10 R_{\odot}$ by a factor of 2, but agree, approximately at $R = 4 R_{\odot}$. Blackwell's data from $R = 6$ to $10 R_{\odot}$ are lower than both the photoelectric and photographic results, but the brightness ratio between equator and poles is in fair agreement with the photographic data.

The polarization data obtained photoelectrically, however, are not in agreement with other work. At the inner edge of the region of the region covered, the tangential component was brighter than the radial, as it should be for the K-corona, where the scattering is by electrons. From $R = 5$ to $11 R_{\odot}$, however, the polarization was in the opposite sense to that measured by others, although the magnitude was not measured. It is unlikely that this negative value of polarization is correct, although negative polarization in the corona has been reported by Öhman. At the present time we have no

explanation for this result. The laboratory calibrations were of an accuracy sufficient to rule out a calibration error. A drift in photomultiplier sensitivity during flight was unlikely, and there was an internal check on amplifier drift.

Pictures of the corona were reconstructed from the photoelectric coronagraph records, and are reproduced in Fig. 17. To accomplish this, the telemeter records, received on magnetic tape, were unscrambled, converted from logarithmic to linear, and used together with a synchronization signal indicating the position in the scan to modulate a lamp; the resulting lamp with intensity was proportional to the instantaneous coronagraphic signal. The light from the lamp was made parallel with a lens, and allowed to fall on a pair of sectored discs like those used in the rocket coronagraph. Another lens imaged the discs on a photographic film. This amounted to a playback of the coronagraph signals through nearly the exact coronagraph in such a way as to produce a photographic image of the actual corona observed in flight. When the motor drove the scanning discs, in synchronization with the lamp modulation produced by the magnetic tape, the sector aperture traced out its spiral, as shown in Fig. 2, and produced the photographs of Fig. 17. A correction had to be introduced, to allow for the rotation of the instrument

caused by the rocket yaw cone. This was done by rotating the photographic film properly, as the spiral scan took place. As a result, the occulter support arm shadow is curved. The sharp arm shadow is that of the arm inside the reproduction instrument, supporting the sectored disc. The diffuse-edged shadow is that caused by this support during flight, and was present in the telemeter record. In the image reconstruction the two shadows should have been placed to coincide. Another correction was introduced to allow for the vignetting function.

The pictures of Fig. 17 agree qualitatively with the isophots of Fig. 16. They show much more detail, some of which is probably real. The very fine mottling is only noise in the photomultiplier output and the effect of the gears driving the discs. The isolated bright spots, or arcs, are thought to be produced by foreign material entering the field of view, such as appears on the photographs of Fig. 11. There is, however, a patch in the east that may possibly be a coronal streamer.

The difference in the radial and tangential pictures between N and S is qualitatively what would be expected.

The radial picture should contain little K-corona, and should therefore be more nearly of the same brightness over the two poles than the tangential picture, which contained a large fraction of the K-corona. The latter seems brighter over the south pole than over the north, like Fig. 12.

CONCLUSIONS:

The rocket experiments of June 28, 1963 have resulted in the first records of the brightness of the solar corona from $R=4$ to $10 R_{\odot}$ made without the aid of a total solar eclipse. The results are far from all that is desired. The most important improvement is to fly in a larger vehicle so that the external occulter can be placed farther away.

It is clear that the moon is the perfect occulter and can never be matched. It is probable, however, that with a multiplier disc occulter, at 10 or more feet from the objective, an orbiting coronagraph will be able to monitor the white light corona with at least as great resolution and sensitivity as can be realized from the ground during a total eclipse.

REFERENCES

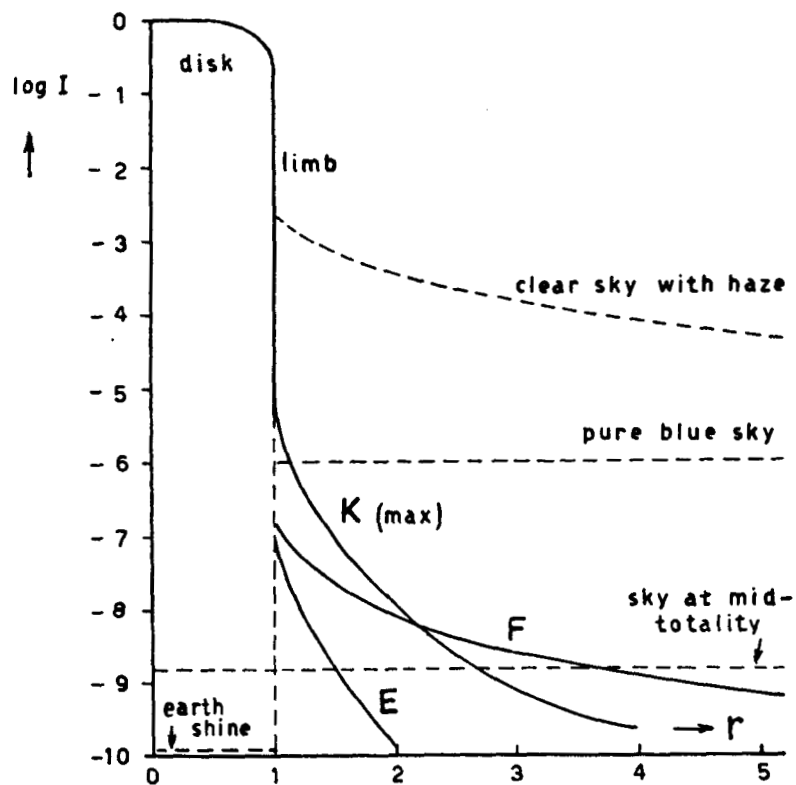
- D. E. Blackwell, Mon. Not. Roy. Astron. Soc. 115, 44, 1955;
116, 56, 1956.
- A. Dolfuss, Compt. rend. 249, 2722, 1959.
- J. W. Evans, J. Opt. Soc. Am. 38, 1083, 1948.
- J. W. Firor, High Alt. Obs., Boulder, Colo.,
private communication, 1964.
- F. Gillette, Summary Report, Jan. 1961 - Dec. 1961,
Atmospheric Physics Program, Univ. of Minnesota.
- H. C. van de Hulst, "The Sun" Ed. G. P. Kuiper,
Univ. of Chicago Press, Chicago, Ill., 1953.
- B. Lyot, Compt. rend. 191, 834, 1930; 193, 1169, 1931;
Mon. Not. Roy. Astron. Soc. 99, 580, 1939;
Ann. Obs. Meudon 8, 1, 1929.
- R. Michard, A. Dolfuss, J.-C. Pecker, M. Laffineur, and
M. d'Azambuja, Ann. d'Astrophys. 17, 320, 1954.
- G. Newkirk, Jr., Sky and Telescope 24, 35, 1962.
- G. Newkirk, Jr., and D. Bohlin, Appl. Optics 2, 131, 1963.
- G. Newkirk, Jr., and D. Bohlin, Appl. Optics, to be
published, 1964.
- G. Newkirk, Jr., and J. A. Eddy, Sky and Telescope
24, 77, 1962.
- Y. Öhman, Stock. Obs. Ann. 15, No. 2, 1947; 18, No. 8,
1955.
- J. D. Purcell, and M. J. Koomen, J. Opt. Soc. Am. 52,
596, 1962.
- G. Wlérick, and J. Axtell, Astrophys. J. 126, 253, 1957.

LIST OF CAPTIONS

- Figure 1. Brightness values, relative to the mean solar brightness, of the several components of the corona (van de Hulst).
- Figure 2. The optical system of the white light coronagraph for OSO-B.
- Figure 3. The two scanning discs for the coronagraph. When placed one over the other and driven by a single spur gear, the point of intersection of the radial and spiral slots scans the corona in a path described by an Archimedes spiral. The corona is covered to $10 R_{\odot}$ in a spiral of 60 turns.
- Figure 4. Teeth cut on the edge of the external occulter keep the diffracted light out of its shadow. Since the light is diffracted at right angles to the edges of the teeth, it is sent into a region bounded internally by a cylindrical envelope, as shown.
- Figure 5. Three exposures of the diffraction pattern produced by a pair of straight edges intersecting at 30° , illuminated by a distant point source. The light is diffracted almost entirely at right angles to the edges.
- Figure 6. Long and short exposures of the shadow cast by smooth and toothed discs, illuminated by a distant point source. The diameter of the discs was 1.32 inches, and the distance to the photographic film was 24 inches. The smooth disc sends much light into the shadow, and the central spot is formed by the focussing action of the intersecting rays. The shadow of the toothed disc is very dark.

- Figure 7. Photographs of the smooth and toothed discs, made with a camera focussed on the discs and with lens placed in the shadow. The arrangement was as in Fig. 5, except that the film was replaced by the camera lens. The smooth disc is bright. Most of the teeth show faintly, because it was impossible to remove all traces of dirt from the edges.
- Figure 8. The distribution of light within the shadow for the smooth and toothed disc, measured with a photomultiplier behind a small aperture. Because the measurements were made in air rather than in vacuum, a considerable amount of light enters the shadow in the region outside the 10 mm position.
- Figure 9. Calibration curves for the photoelectric coronagraph, made in the vacuum tank.
- Figure 10. The computed vignetting function for the photographic coronagraph, and the illumination in the focal plane expected to be produced by the corona.
- Figure 11. The photographs of the corona obtained on June 28, 1963. Solar north is at the top of each picture and east at the left. During the longer exposures the image rotated due to rocket yaw, as indicated by the position of the arm supporting the occulter. Because of misalignment one edge of the occulter shone with diffracted light. Bright spots of the type present on all the pictures were from foreign matter, dislodged during takeoff, and coming to rest on the field lens. The many tracks, indicated by letters, are of small objects in space. Their entrance into the field of view and exit are noted by arrows, and each letter refers to a particular object.
- Figure 12. The solar corona on June 28, 1963. - The original of Exposure No. 11, and a print from which the artifacts and spurious objects have been removed by retouching the corona photographed by the High Altitude Observatory during the total eclipse of July 20, 1963 is introduced at the proper scale and orientation.

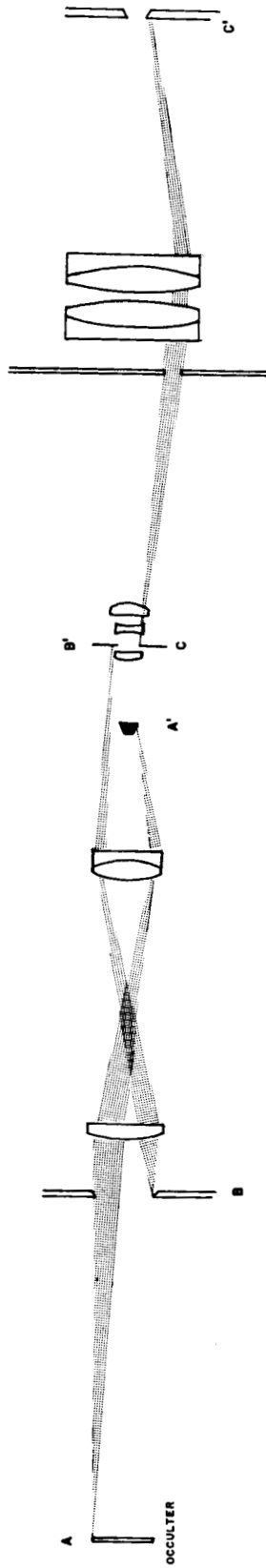
- Figure 13. The brightness of the corona, June 28, 1963, as determined from Photographs 1, 11, and 20. The brightnesses, in ft. -Lamberts, may be converted to fractions of the mean solar brightness by multiplication by 1.4×10^{-8} .
- Figure 14. The distribution of brightness in the corona - average values determined from the isophots of Fig. 13.
- Figure 15. The brightness of the corona as determined photoelectrically June 28, 1963 - average values.
- Figure 16. The brightness of the corona on June 28, 1963, as recorded by the photoelectric coronagraph in radial and tangential polarization (vibration).
- Figure 17. Photographs of the corona in radial and tangential polarization, reconstructed from the data telemetered from the photoelectric coronagraph.



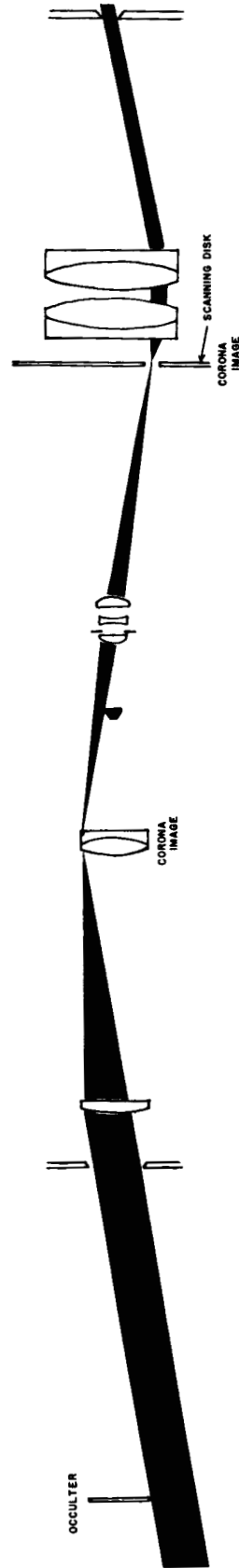
Relative intensities of the components of coronal light: K = continuous light due to electron scattering; F = inner zodiacal light; E = combined light of emission lines.

Figure 1

RELAY CORONAGRAPH



TRAPPING OF DIFFRACTED SUNLIGHT



IMAGING OF SOLAR CORONA

Figure 2

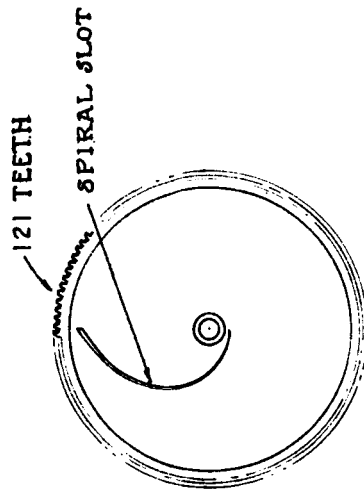
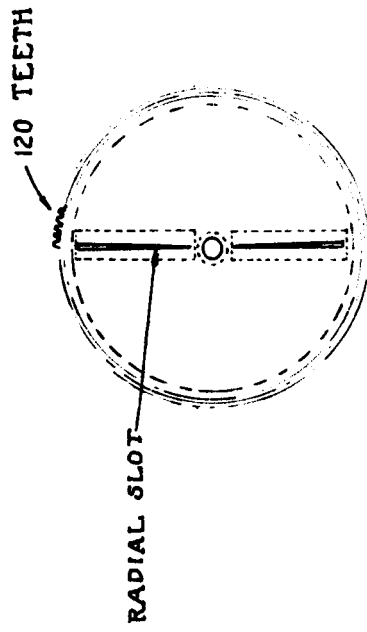
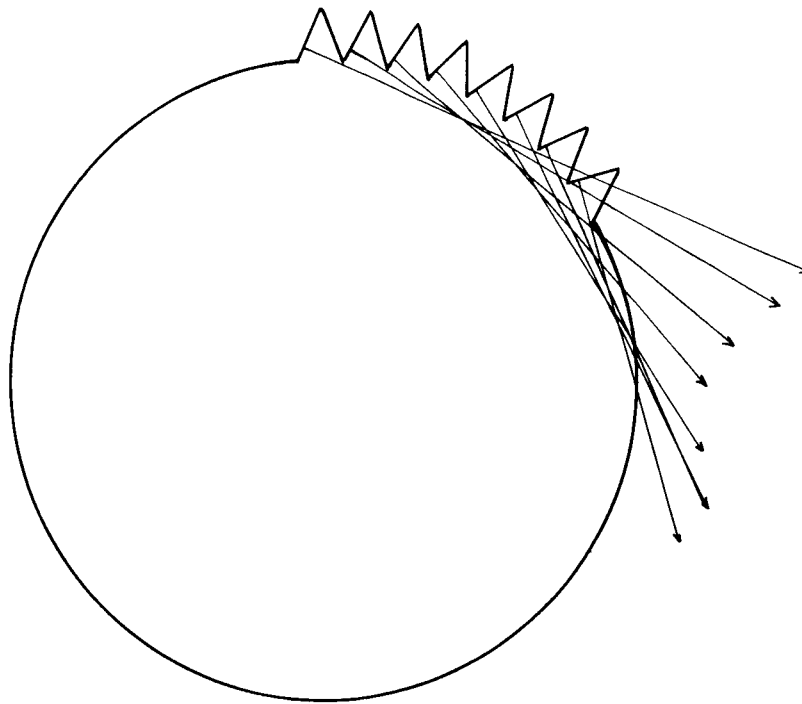


Figure 3



DIRECTION OF DIFFRACTED LIGHT
SAWTOOTH DISK

Figure 4

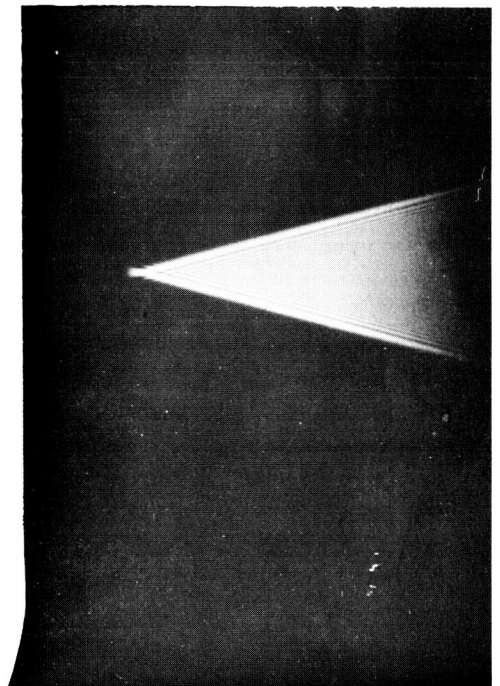
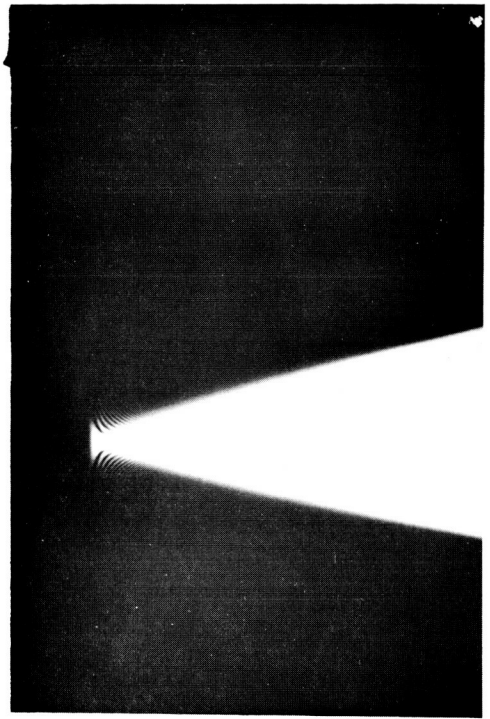
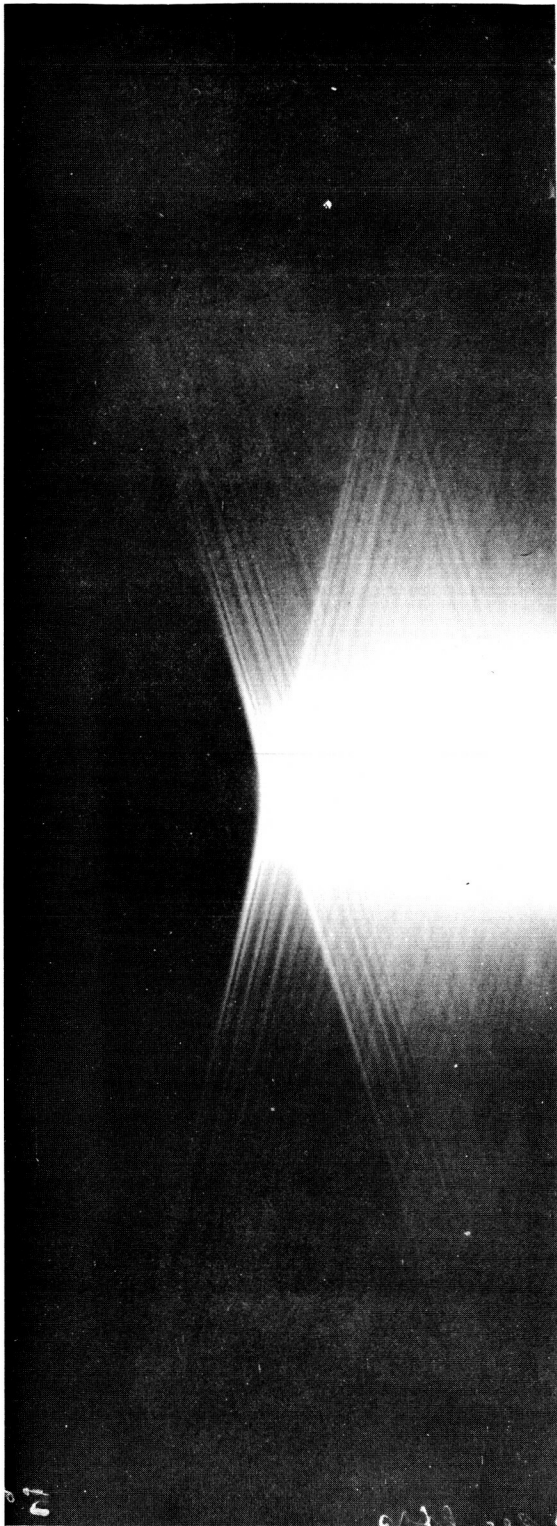


Figure 5

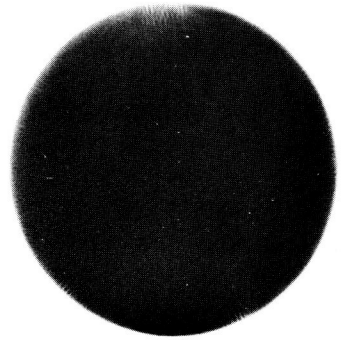
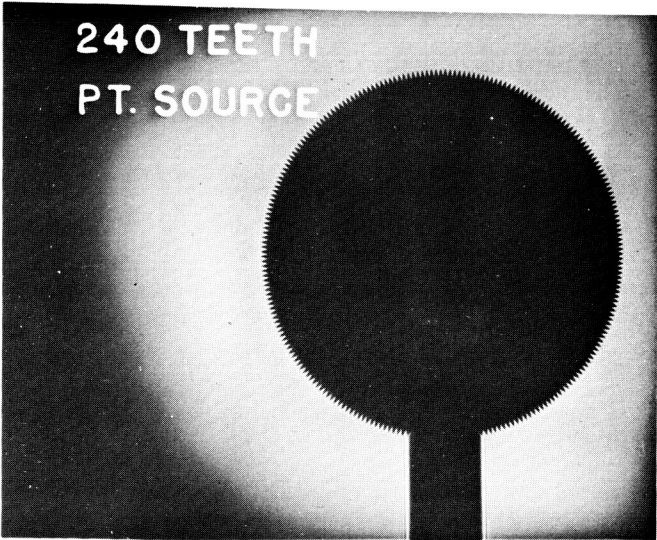
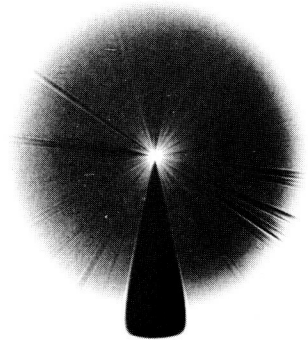
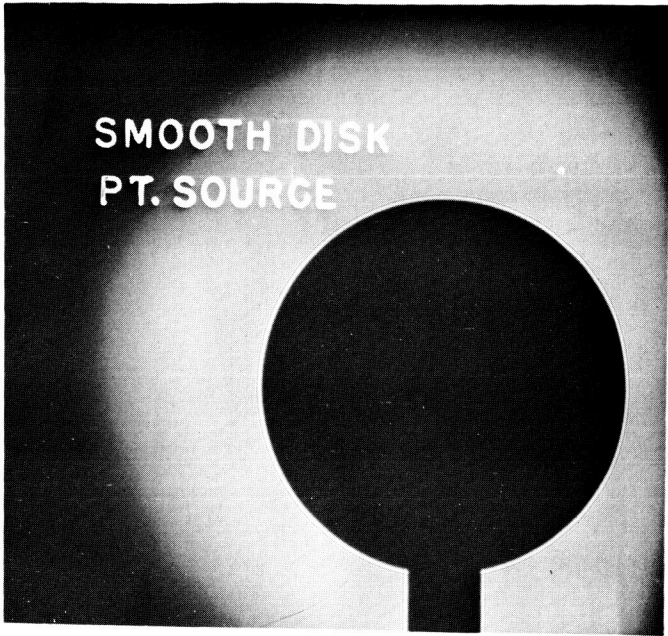


Figure 6

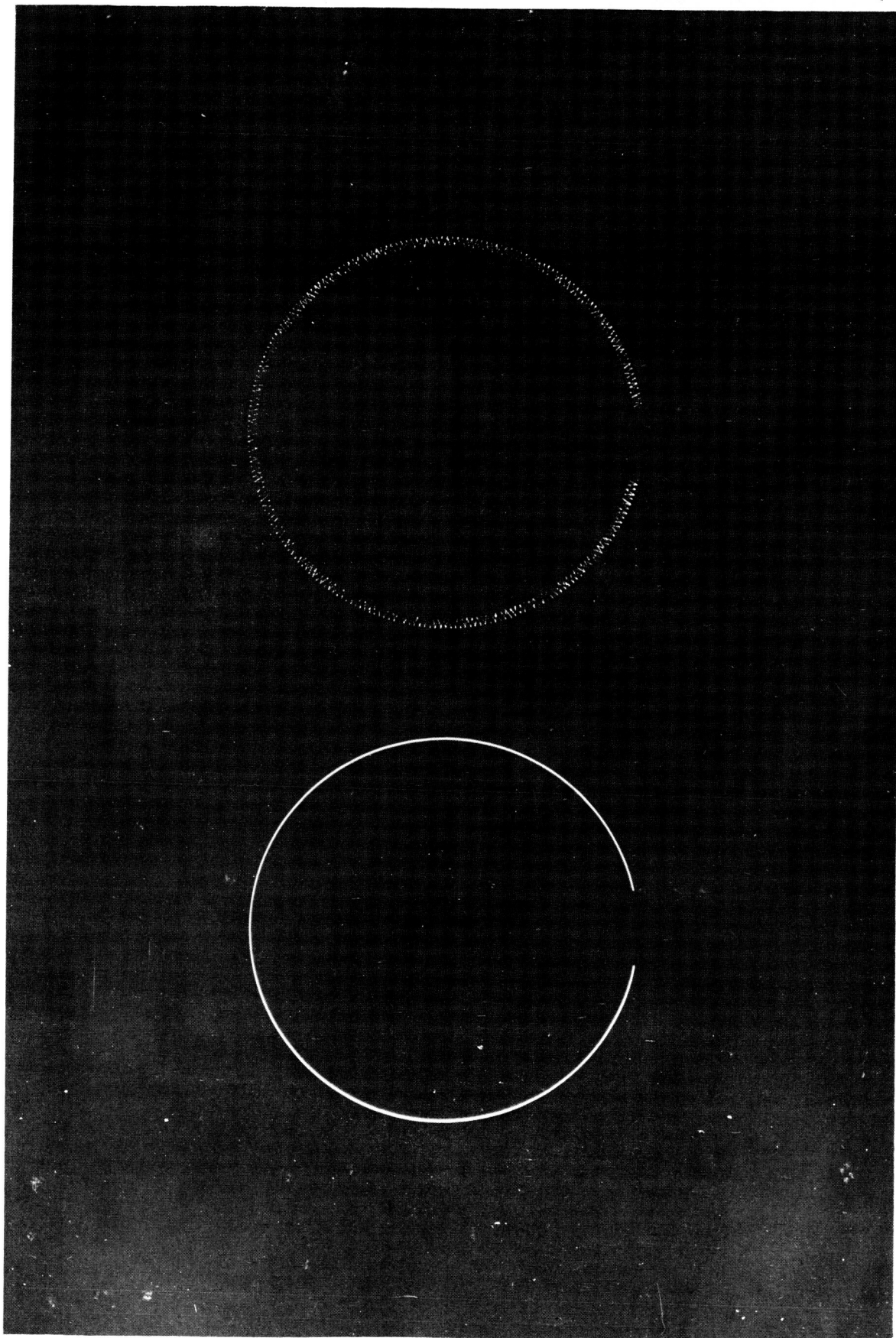


Figure 7

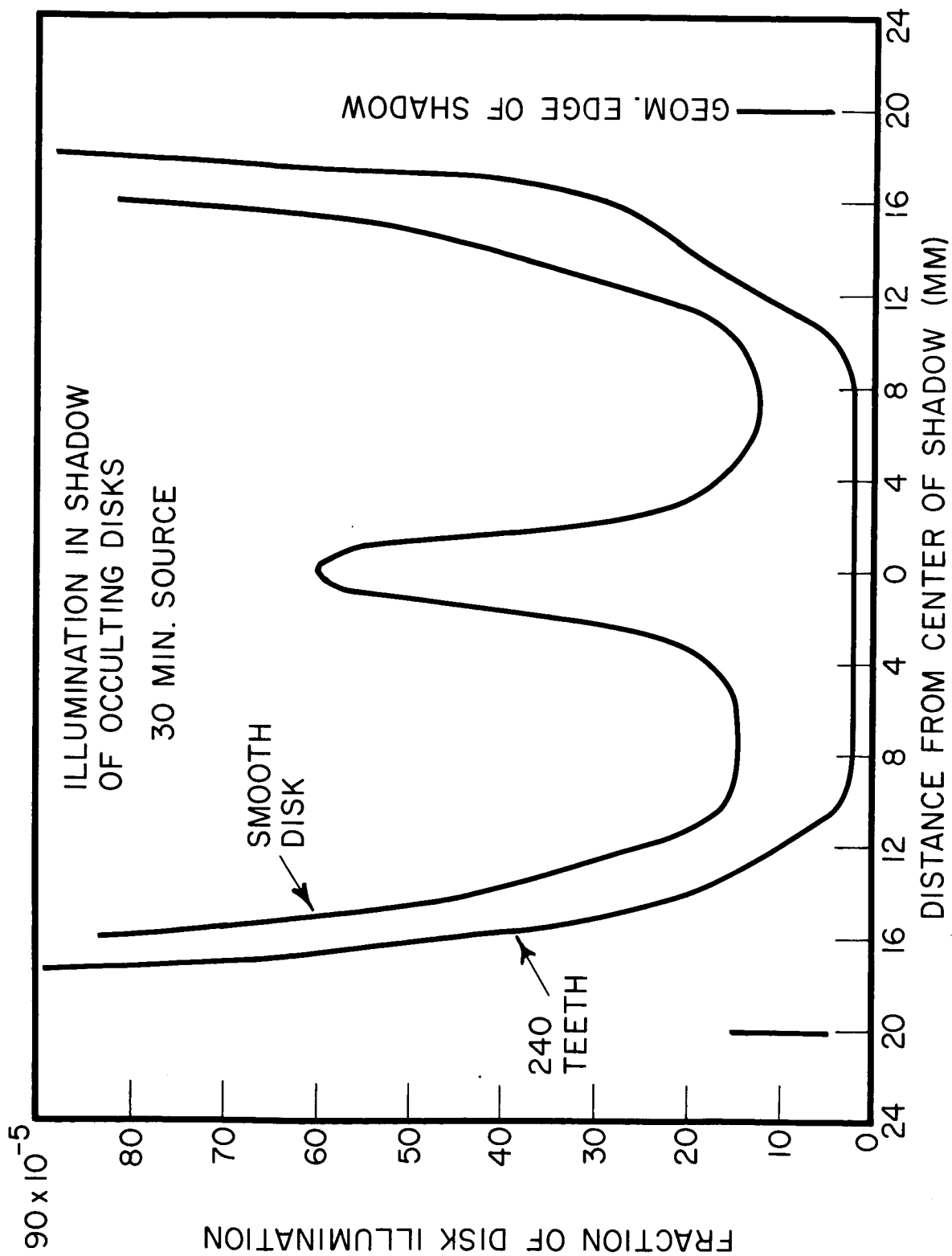


Figure 8

PHOTOELECTRIC CORONAGRAPH
 LAUNCHED JUNE 28, 1963
 7:30 AM MST

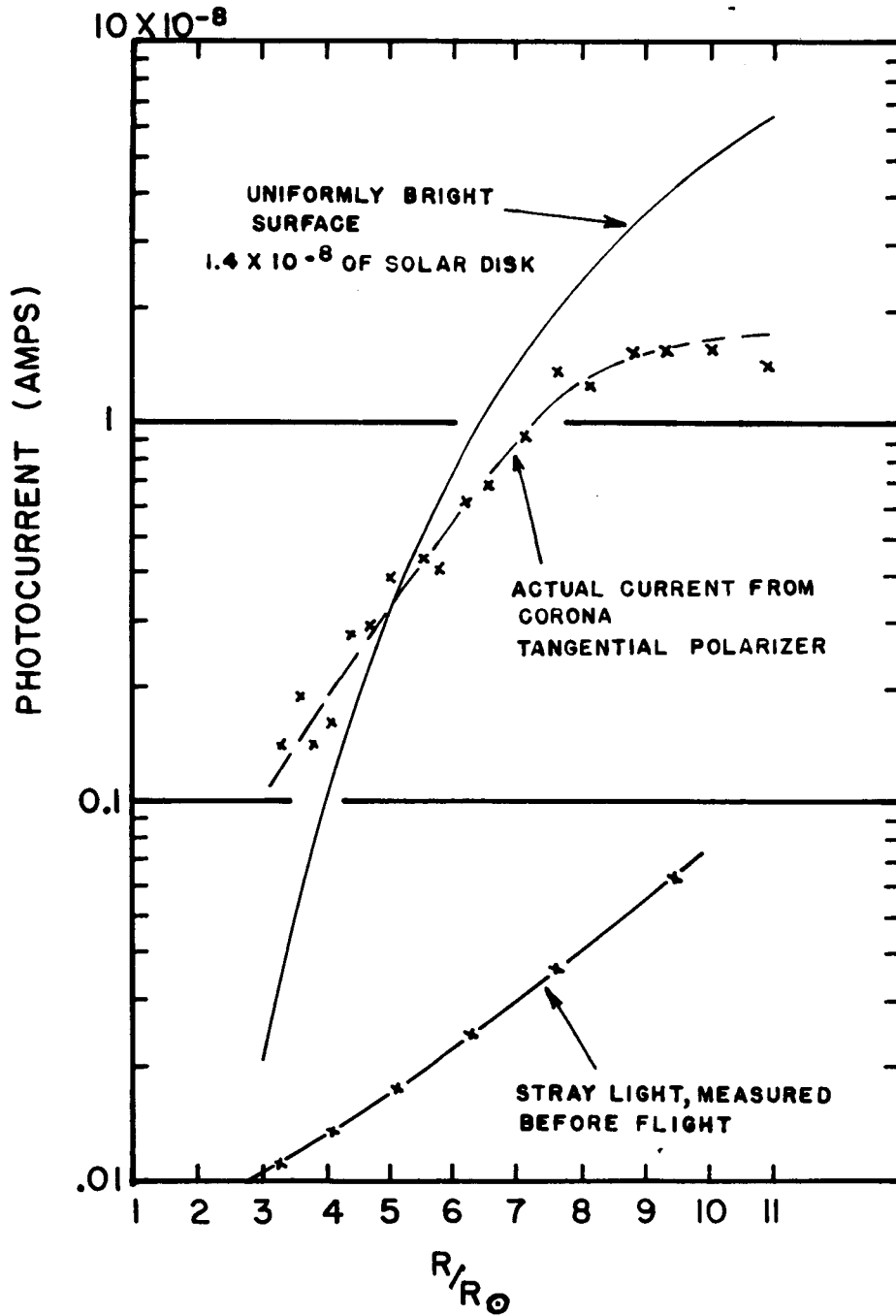


Figure 9

COMPUTED VIGNETTING OF
 PHOTOGRAPHIC CORONAGRAPH
 LAUNCHED 28 JUNE 1963

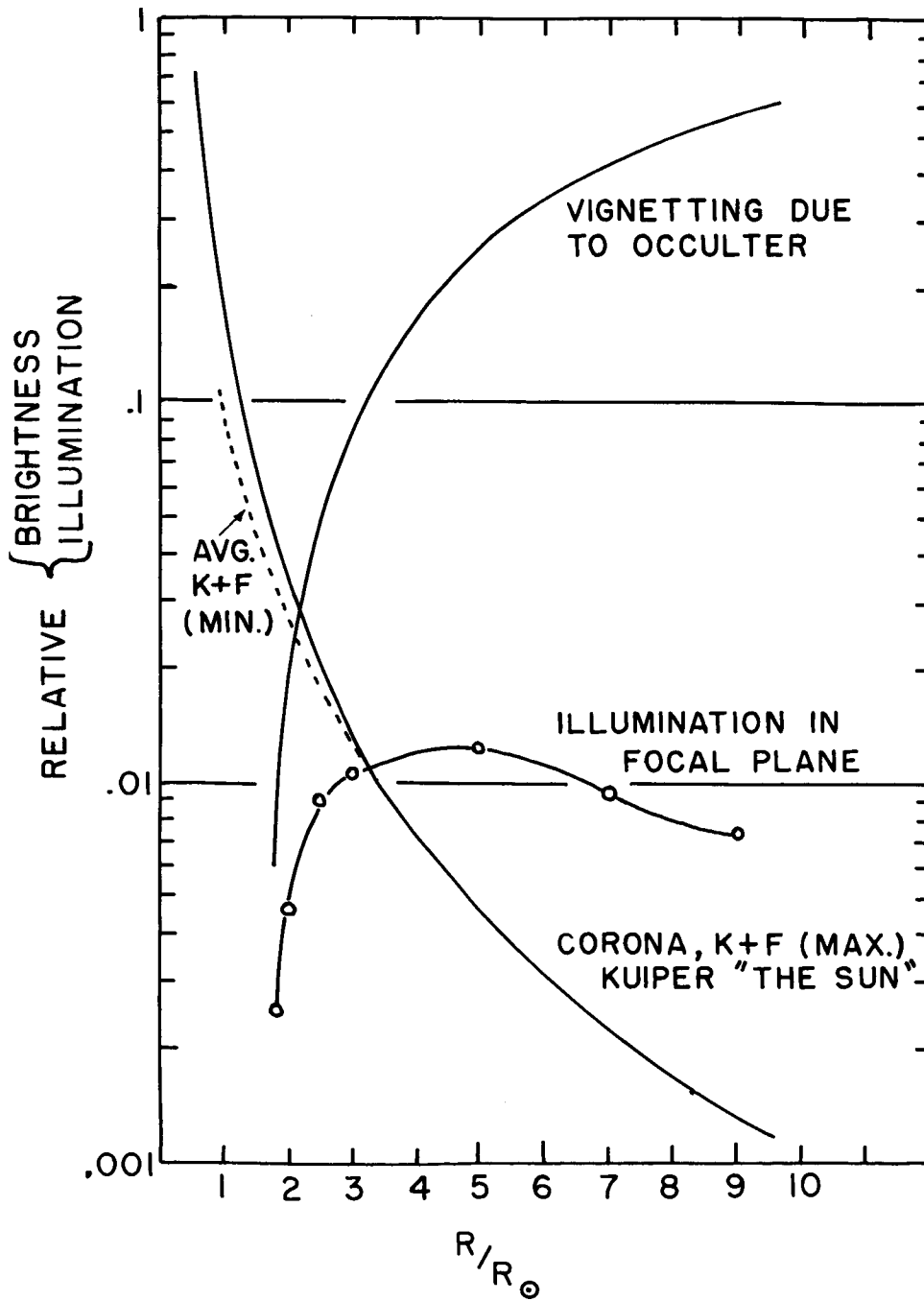


Figure 10

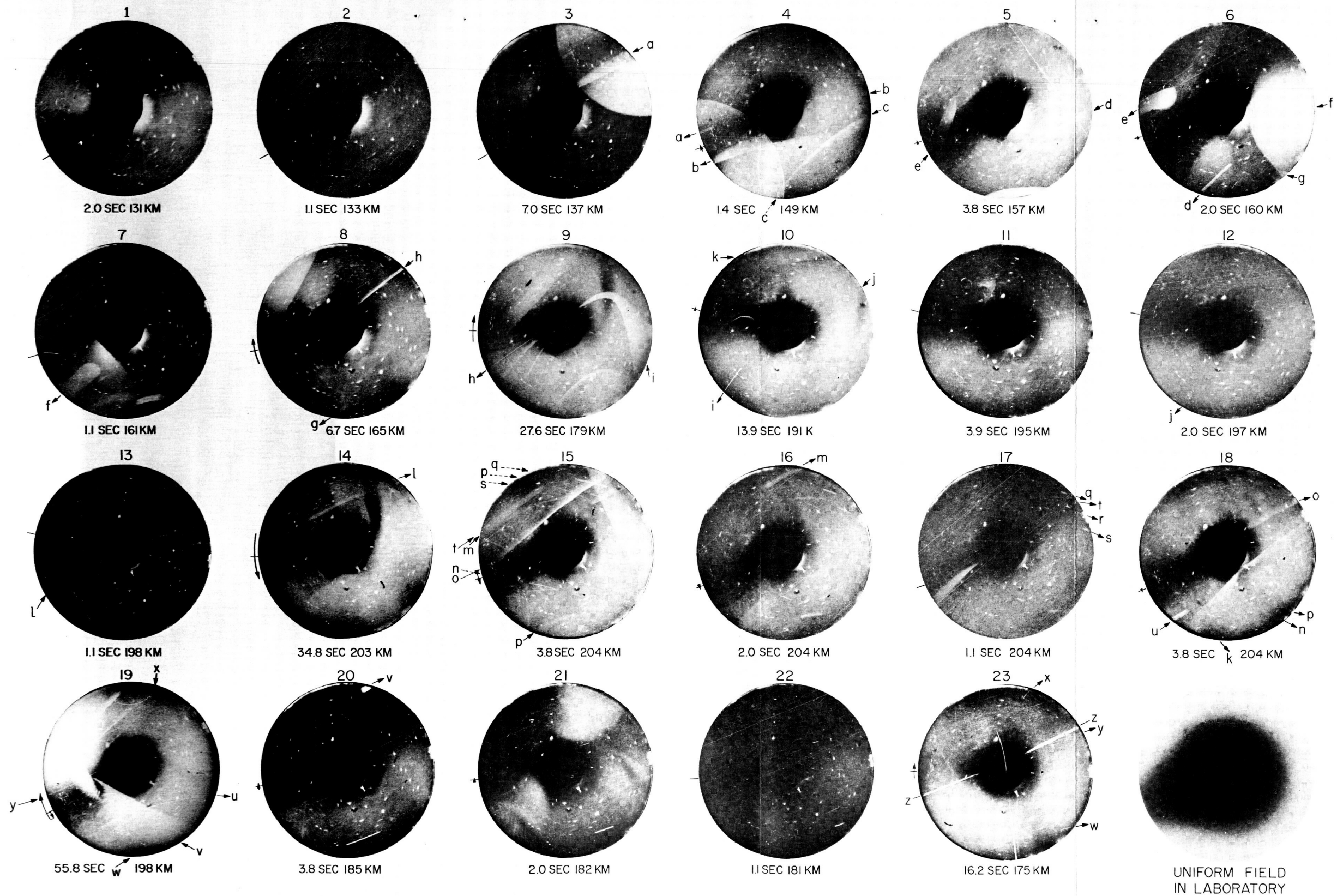
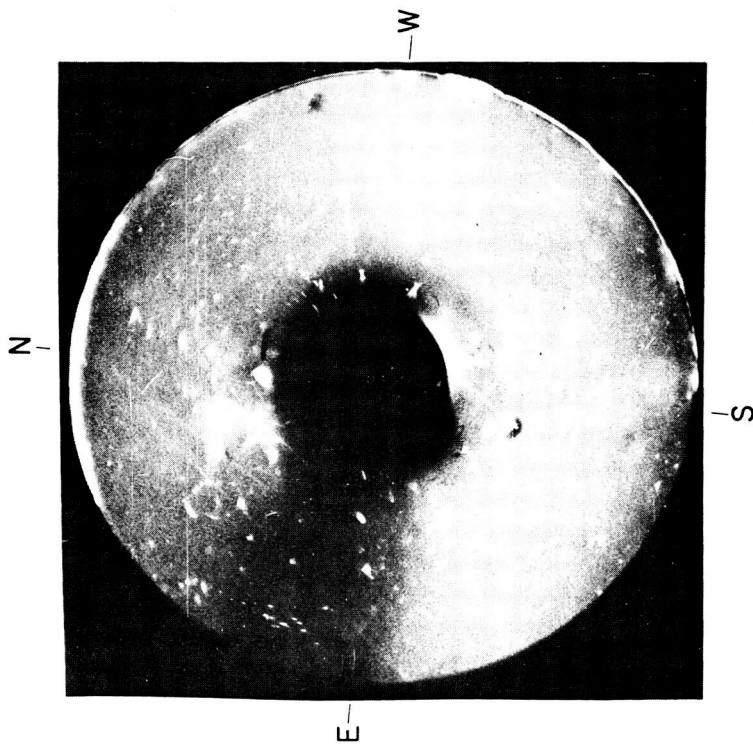
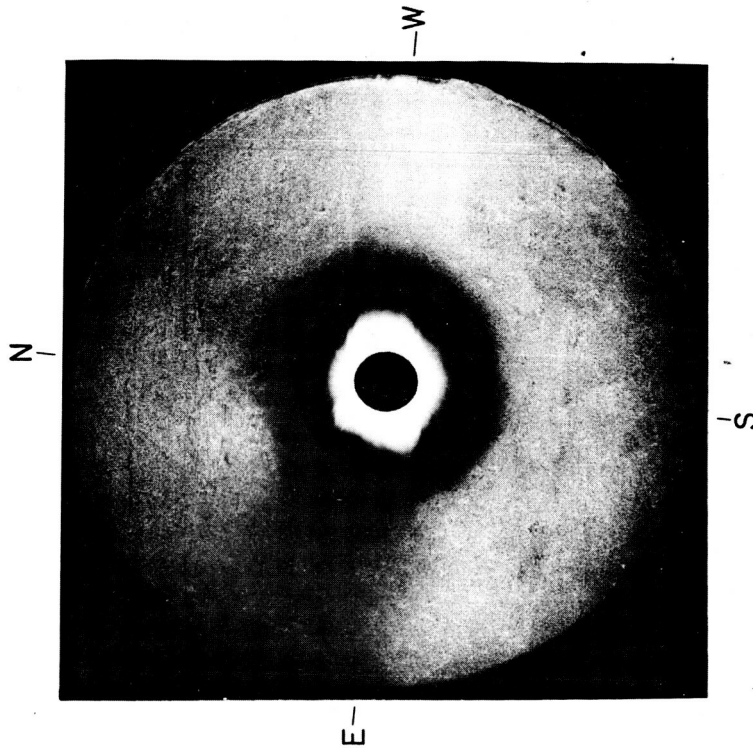
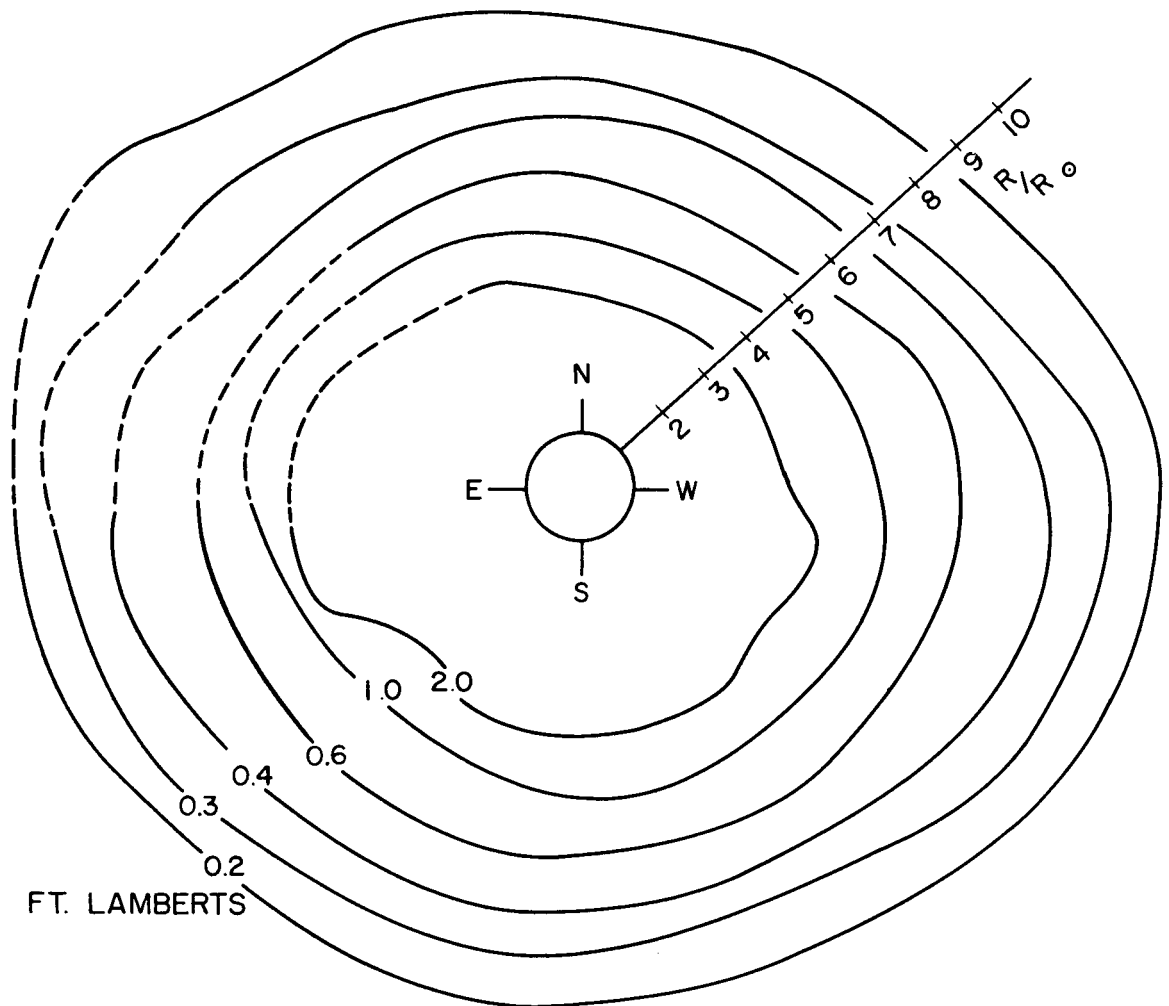


Figure 11



THE WHITE LIGHT CORONA OF THE SUN
PHOTOGRAPHED FROM AN AEROBEE-HI ROCKET
U. S. NAVAL RESEARCH LABORATORY
JUNE 28, 1963

Figure 12



ISOPHOTS FOR K+F CORONA
 DATA FROM FOUR PHOTOGRAPHS
 JUNE 28 1963
 AEROBEE NE 3.129

Figure 13

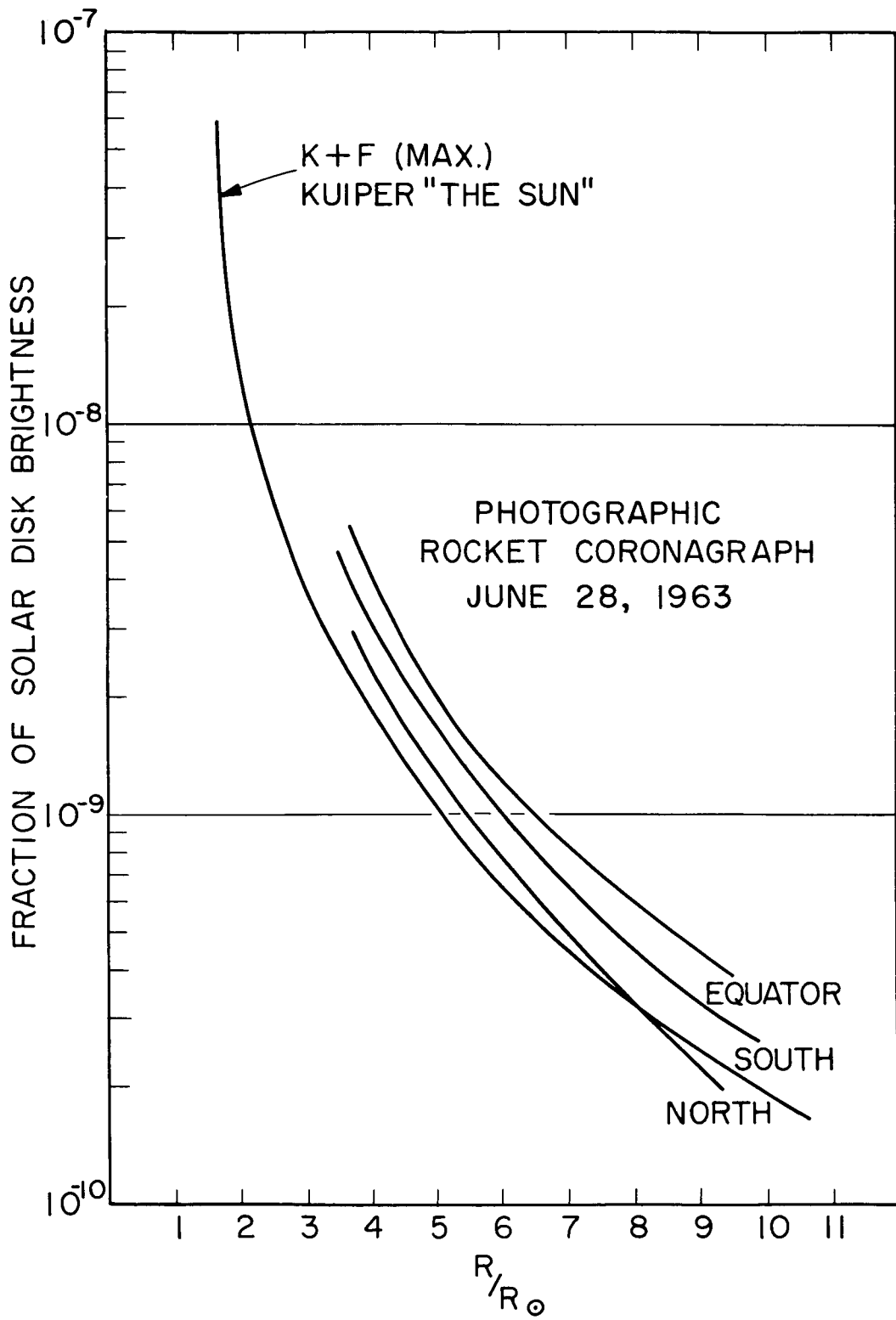


Figure 14

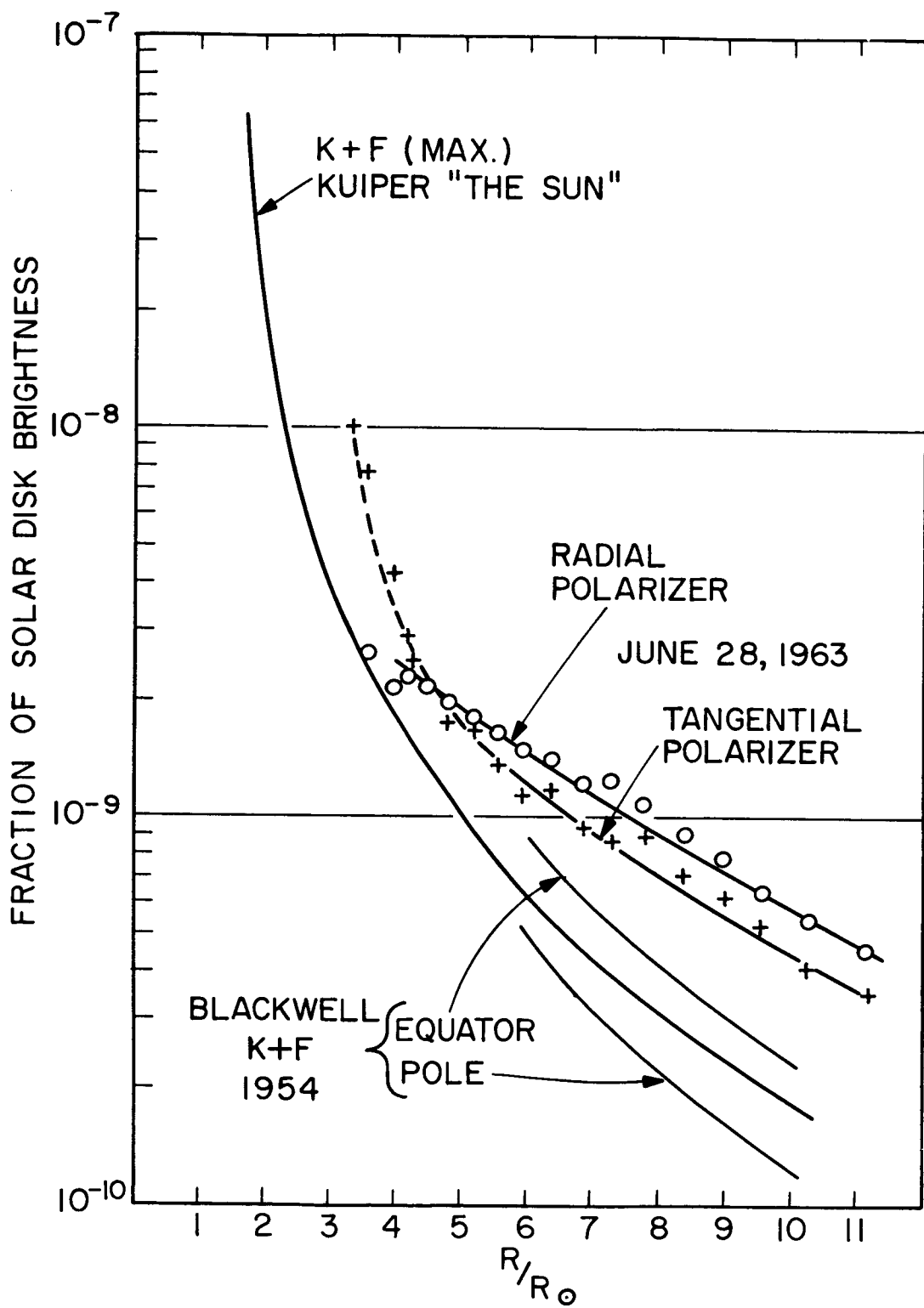
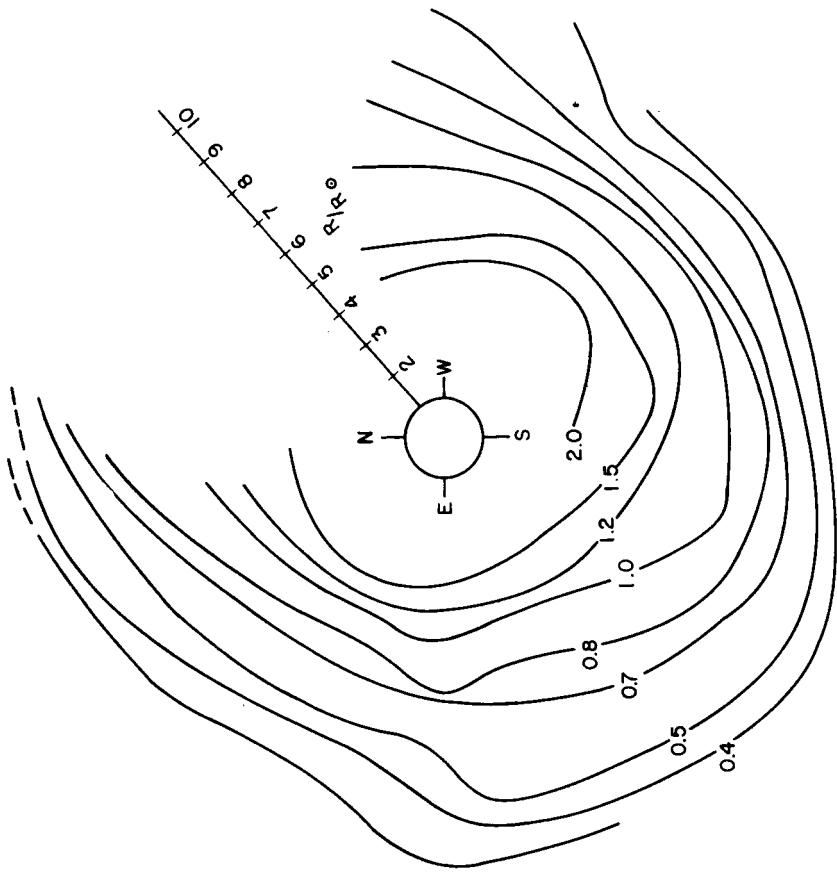


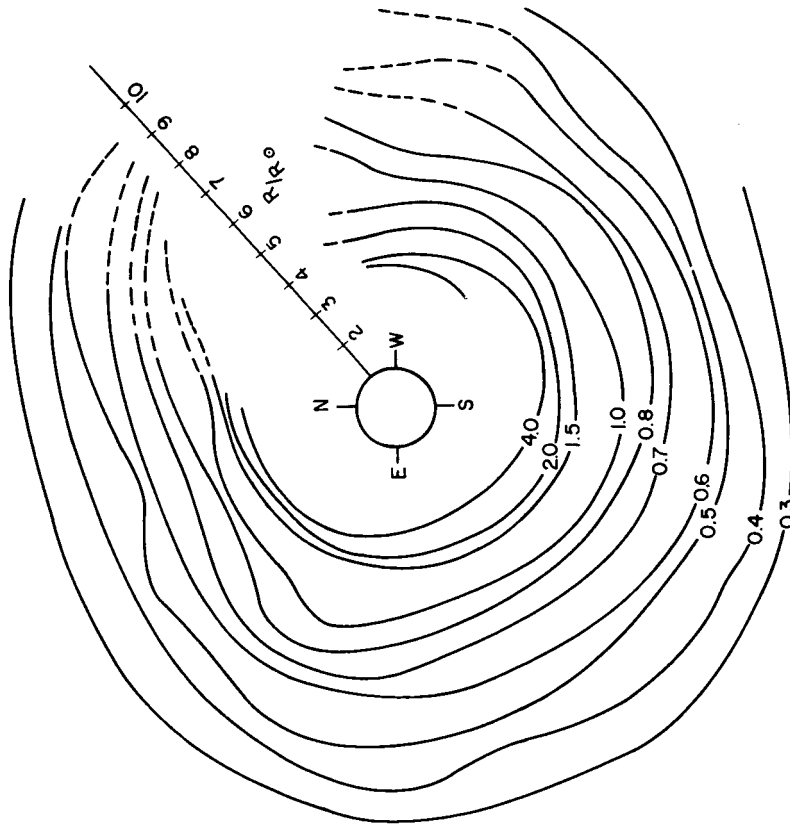
Figure 15

PHOTOELECTRIC CORONAGRAPH
AEROBEE NE 3.129
28 JUNE 7:30 MST



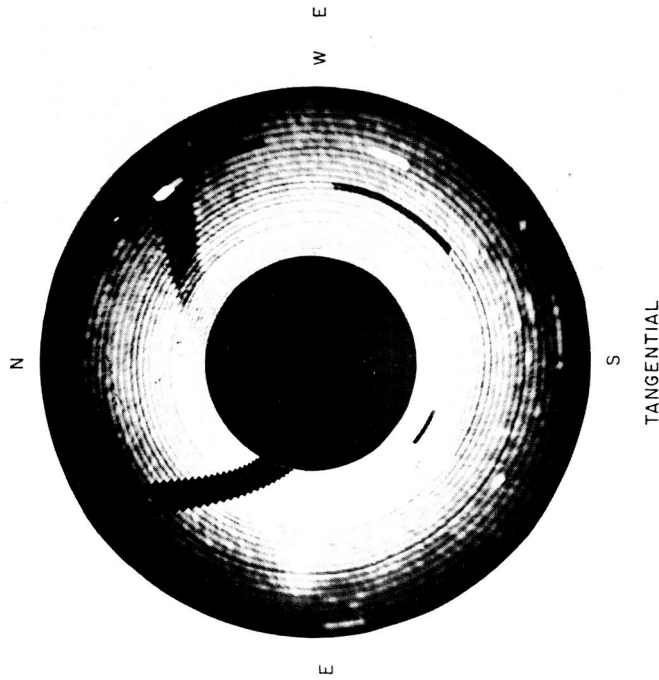
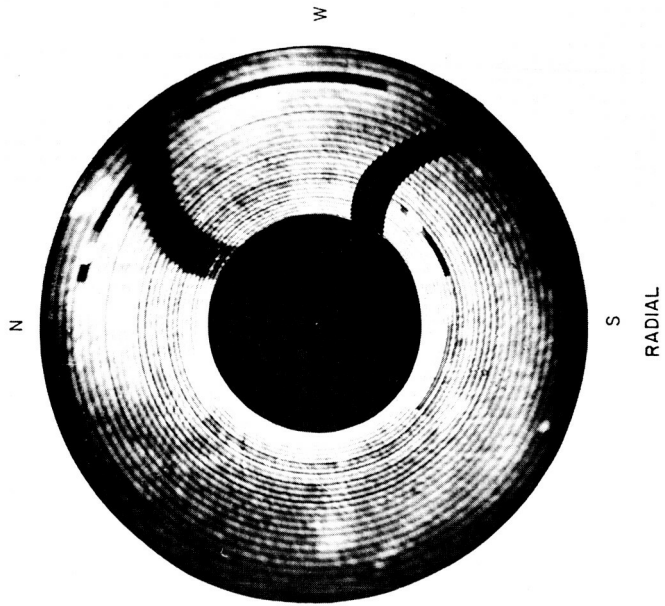
ISOPHOTS (FT LAMBERTS)

RADIAL POLARIZER



TANGENTIAL POLARIZER

Figure 16



THE CORONA AS RECONSTRUCTED FROM THE TELEMETER RECORDS
JUNE 28, 1963

Figure 17